

AN ABSTRACT OF THE THESIS OF

Jan E. True for the degree of Master of Science in Chemistry presented on April 6, 1999.

Title: Electronegativity of $-\text{SF}_5$, $-\text{CF}_3\text{SO}_2$, and $-\text{SO}_2\text{F}$ Measured with X-ray Photoelectron Spectroscopy.

Redacted for Privacy

Abstract approved: _____

John Westall for T. Darrah Thomas

The electronegativities of $-\text{SF}_5$, $-\text{CF}_3\text{SO}_2$, and $-\text{SO}_2\text{F}$ have been measured with gas phase X-ray photoelectron spectroscopy. Of these three groups previously measured values were found only for $-\text{SF}_5$. The electronegativities of $-\text{Cl}$, $-\text{Br}$, $-\text{CH}_3$, and $-\text{CF}_3$ were concurrently measured to determine how the findings of this research compare with other experimental values found in the literature. Our experimental electronegativities for $-\text{SF}_5$, $-\text{CF}_3\text{SO}_2$, and $-\text{SO}_2\text{F}$ are 2.81 ± 0.12 , 2.49 ± 0.09 , and 2.92 ± 0.12 respectively. The electronegativity of $-\text{CF}_3$ currently measured (2.78 ± 0.08) is significantly lower than other experimental values. The electronegativity of $-\text{SF}_5$ is in agreement with other experimental values.

The experimental electronegativities are compared with theoretical values calculated based on the assumption of Electronegativity Equalization and based on Mulliken's definition of electronegativity. It is found that the electronegativities calculated with Electronegativity Equalization are higher than the experimental values currently measured, and those calculated with Mulliken's definition are lower than the experimental values.

Electronegativity of $-\text{SF}_5$, $-\text{CF}_3\text{SO}_2$, and $-\text{SO}_2\text{F}$ Measured
with X-ray Photoelectron Spectroscopy

by

Jan E. True

A THESIS

submitted to

Oregon State University

in partial fulfillment of
the requirements for the
degree of

Master of Science

Presented April 6, 1999
Commencement June 1999

Master of Science thesis of Jan E. True presented on April 6, 1999

APPROVED:

Redacted for Privacy

Major Professor, representing Chemistry

Redacted for Privacy

Chair of Department of Chemistry

Redacted for Privacy

Dean of Graduate School

I understand that my thesis will become part of the permanent collection of Oregon State University libraries. My signature below authorizes release of my thesis to any reader upon request.

Redacted for Privacy

Jan E. True
Jan E. True, Author

ACKNOWLEDGEMENTS

My first contact with Dr. T. Darrah Thomas came when I took Physical Chemistry from him as an undergraduate. The subject of that term was Thermodynamics. Darrah's ability to make simple and understandable ideas out of what could be very complicated subject matter kindled a passion and yearning in myself to delve deeply into the content of Physical Chemistry. This experience only deepened as I had the pleasure of taking an additional quarter of Physical Chemistry from him, with the subject of that term being Quantum Mechanics. Gratefully for me I have had the opportunity to experience this with a master of these subjects. It has been an incredible pleasure and honor to work with a person of the intelligence and scientific insights of Dr. Thomas.

As like attracts like, I have had the pleasure of working with other Physical Chemists of incredible ability as a result of working with Dr. Thomas. Dr. Thomas Carroll's patience and willingness in answering my many questions has given me much learning and understanding. Although my contact with him has been brief, Dr. Leif Sæthre has also played a major role in furthering my understanding of Physical Chemistry as it relates to XPS. This work and all of the learning it has provided me would not have been possible without the efforts of Dr. Gary Gard, who synthesized the compounds studied in this project.

Finally, I must thank Dr. Phil Siemens, whose support and faith in my scientific abilities gave me the courage to proceed through my graduate work. I don't feel I could have completed this without the experiences I shared with Dr. Siemens, and I am deeply indebted to him.

TABLE OF CONTENTS

	<u>Page</u>
1. INTRODUCTION	1
1.1 Purpose	1
1.2 What is Electronegativity?	2
1.3 Using XPS to Determine Electronegativity	5
2. EXPERIMENTAL PROCEDURES AND DATA ANALYSIS	8
2.1 The Spectrometer	8
2.1.1 The X-ray Source	8
2.1.2 The Cylindrical Mirror Analyzer	12
2.1.3 The Detector	12
2.1.4 Electronics and Computer	13
2.2 Measuring a Spectrum	13
2.3 Data Analysis	16
2.3.1 Determining Peak Positions	16
2.3.2 Calibration	17
3. RESULTS AND DISCUSSION	19
3.1 Electronegativities of $-\text{SF}_5$, $-\text{CF}_3\text{SO}_2$, and $-\text{SO}_2\text{F}$	19
3.2 Comparison of $-\text{SF}_5$ Electronegativity from C 1s and S 2p Data	28
3.3 Correlation with Modified Sanderson Calculations	29
4. CONCLUSIONS	35
REFERENCES	37
APPENDIX	40

LIST OF FIGURES

<u>Figure</u>	<u>Page</u>
2.1 Cross section view of Oregon State University spectrometer main components	9
2.2 Cross section view of gas cell and major x-ray tube components	10
2.3 SF ₅ CH ₃ CH ₃ C 1s and S 2p spectra with the simultaneously measured Ne 1s and Ne 2s spectra	15
2.4 Plot of Ne 1s and Ne 2s calibrants from which B and C can be calculated for each spectrum	18
3.1 Plot of core-ionization energy shifts calculated using Eqn. 3.1 versus measured core-ionization energies	21
3.2 Graphic representation of Eqn. 3.2 used to calculate electronegativities (χ_i) from c coefficients (c_i)	22
3.3 Plot of measured ionization energies against Equivalent cores and Koopman's theorem energies	27
3.4 Sulfur 2p ionization energies versus electronegativity of group X	29
3.5 Plot of currently measured C 1s IE shifts versus atomic charge calculated with modified Sanderson method	34

LIST OF TABLES

<u>Table</u>		<u>Page</u>
3.1	Experimental electronegativities (Pauling units)	23
3.2	Experimental electronegativities compared with calculated values (Pauling units)	24
3.3	SF ₅ X S2p ionization energies and halogen electronegativities (χ) used to calculate the electronegativity of -SF ₅	29
3.4	Calculated atomic charges on carbon for gas phase molecules and the corresponding currently measured C1s IE shifts	33

LIST OF APPENDIX TABLES

<u>Table</u>		<u>Page</u>
1	Experimental core-ionization energies, including the date the compound was ran and the spectrometer constant	41
2	Experimental core-ionization energies used to determine electronegativities, their shifts relative to methane, core-ionization energies calculated using Equation 3.1, and the substituent composition of each compound	44

This thesis is dedicated to Jenny, Raeanne, Harris and Peggy
- my companions and fellow journeyers

Electronegativity of $-\text{SF}_5$, $-\text{CF}_3\text{SO}_2$, and $-\text{SO}_2\text{F}$ Measured with X-Ray Photoelectron Spectroscopy

1. INTRODUCTION

1.1 Purpose

The concept of electronegativity was introduced in the 1930's. Around that time Pauling¹ defined an electronegativity scale for elements that is still used. Pauling defined electronegativity as the power of an atom in a molecule to attract electrons to itself.¹ An electronegativity scale for group substituents could provide useful insights into the reactivities and physical properties of molecules containing such groups. It is the goal of this research to determine electronegativity values for $-\text{CF}_3\text{SO}_2$, $-\text{SF}_5$, and $-\text{SO}_2\text{F}$ groups within organic molecules using core-ionization energies obtained through gas phase X-ray photoelectron spectroscopy (XPS). These substituents are of chemical interest because they can perhaps provide insight into the effects of electron withdrawing power and polarizability on electronegativity.

Many quantitative methods have been proposed for calculating group electronegativities. The modified Sanderson method, described in section 3.3, provides a simple model for calculating group electronegativities. Sanderson equated stability ratios and partial charges with electronegativity. The correlation between currently measured carbon 1s ionization energies (linearly related to electronegativities as described in section 1.3) and partial charges calculated with the modified Sanderson method is determined.

1.2 What is Electronegativity?

In addition to the many quantitative methods proposed for calculating electronegativities, many qualitative definitions of electronegativity have also been proposed.² The description of electronegativity proposed by the pioneering authors Pauling and Mulliken are reviewed here. Pauling described bonds such as A-A and B-B as normal covalent bonds and postulated that the bond energy $D(A-B)$ between unlike atoms would always be greater than the bond energy $D(A-A)$ and $D(B-B)$ in bonds between like atoms.³ The bond energy $D(A-B)$ between unlike atoms would be greater in energy because of the increased ionic character of the bond. Based on this postulate Pauling defined Δ as the following difference

$$\Delta = D(A-B) - \frac{1}{2}\{D(A-A) + D(B-B)\} \quad (1.1)$$

which would never be negative if $D(A-A)$ and $D(B-B)$ were always less than $D(A-B)$. Because the alkali halides were one set of compounds which did give negative Δ values, Pauling postulated that Δ may be more properly described with a geometric mean between $D(A-A)$ and $D(B-B)$ than the arithmetic mean as shown in Eqn. 1.1

$$\Delta' = D(A-B) - \{D(A-A)D(B-B)\}^{1/2} \quad (1.2)$$

Pauling recognized that the geometric mean leads to more satisfactory values for normal covalent bonds between unlike atoms, but he also recognized there was only a small difference between the arithmetic and geometric means for cases where $D(A-A)$ and $D(B-B)$ do not differ greatly in value.⁴ Because the Δ values “can be obtained directly from heats of reaction, whereas knowledge of individual bond energies is needed for the calculation of values of Δ' ”, Δ is frequently used instead of Δ' to determine electronegativities.

Pauling used the relation

$$\chi_A - \chi_B = 0.208\Delta^{1/2} \quad (1.3)$$

to determine the electronegativities χ_A and χ_B , where the factor of 0.208 is included to convert $(\text{kcal/mol})^{1/2}$ to $(\text{eV})^{1/2}$. Pauling thus calculated an electronegativity value for each atom. With this approach to electronegativity hybridization and atomic charge effects are completely neglected.

Mulliken's definition of electronegativity was based on the premise that the power of an atom in a molecule to attract electrons to itself is proportional to the average of the valence-state ionization potential (IE) and the electron affinity (EA) of the atom⁵, with the electron affinity being defined as the energy released when an atom binds an electron to itself.⁶ The equation Mulliken used to calculate electronegativities χ is

$$\chi^M = (\text{IE} + \text{EA})/2 \quad (1.4)$$

Mulliken's definition of electronegativity allows for the effects of varying hybridization, with an electronegativity value for each valence state calculated from the appropriate values of IE and EA. The greater the valence state of an atom in a molecule, the greater its electronegativity. For example, Mulliken proposed an electronegativity of 2.15 for the s^2p^3 valence state of N and 2.56 for the sp^3 state (the absolute values have been adjusted to correspond to Pauling's scale.) Pauling proposed the single value of 3.0 for N. Mulliken electronegativity also allows for the effects of charge by using IE and EA values for charged species. Mulliken's electronegativities χ^M are related to Pauling's electronegativities through Eqn. 1.5:

$$\chi = 0.336(\chi^M - 0.615) \quad (1.5)$$

Mulliken's definition of electronegativity has greater theoretical support than Pauling's, but Pauling's definition may have remained the most prevalent because the data needed to calculate Mulliken's electronegativities weren't sufficiently available until the 1960's.² Mullay concludes that Mulliken's description also makes more intuitive sense than does Pauling's: "Each atom attempts to keep one electron (i.e. resist becoming a positive ion) and simultaneously acquire the second electron (i.e. become a negative ion.) These two processes can be seen as involving the ionization potential and electron affinity respectively."²

It is necessary to address the issue of units for electronegativity, for one might expect the units to somehow relate to the meaning of electronegativity. As already noted, Pauling's units are $(\text{energy})^{1/2}$, and it is obvious from Eqn. 1.4 that Mulliken's units are (energy). Electronegativities determined with the Sanderson method as described in section 3.3 are unitless. Most frequently electronegativities are reported as unitless quantities, an exasperation for the seeker of the "true" meaning of electronegativity. Yet comparisons are routinely made between electronegativity values calculated with different methods (as will be done in this paper.) Mullay² notes the suggestion made that there is no meaning to the concept of electronegativity and that therefore the entire notion should be rejected. Mullay counters this suggestion with the statement that "the proven usefulness of the concept and the lack of easily used and inexpensive rigorous quantum mechanical methods makes this position unreasonable."²

A much more recent description of electronegativity has been proposed by Aitken et al.⁷ They describe electronegativity as arising from two related effects: atoms

competing with one another for electrons and the atoms ability to accept positive or negative charge. The first of these is essentially equivalent to Pauling's definition of electronegativity. The second can be related to the polarizability of the atom. Both of these characteristics should then affect the ability of a molecule to accept positive or negative charge through a wide variety of processes such as ionization, protonation, or proton removal. In this work core-ionization energies have been measured to determine group electronegativities of $-\text{CF}_3\text{SO}_2$, $-\text{SF}_5$, and $-\text{SO}_2\text{F}$, i.e., to determine the combined influence of each groups' ability to compete for electrons and to accept charge.

When considering a molecule accepting charge one can view the ability of an atom (or group) to draw electrons to itself as an initial-state effect and the ability to accept charge as a final-state effect.⁷ The ground-state electron distribution in the molecule is mostly determined by the atoms competition for these electrons, hence the label "initial-state effect." Once a new charge has been accepted the polarizability of the atom is most important in determining how the new charge is redistributed, hence the label "final-state effect." Using V to represent the initial-state effect, R for the final-state effect, and χ to represent electronegativity, one might then expect an equation of the form $\chi = V + R$ to describe electronegativity.

1.3 Using XPS to Determine Electronegativity

A classical model will be used to show how core-ionization energies and electronegativities may be related.⁸ The electric potential Φ_q on the atom/group can be expressed as

$$\Phi_q = \Phi_0 - \alpha' q e \quad (1.6)$$

where Φ_0 represents the potential on the atom when its charge, q , is zero and there is therefore no polarization of the area surrounding the site of charge transfer. The constant α' is closely related to the polarizability of the surroundings. This second term represents the effects of the additional charge q . The minus sign is included because a negative charge will induce a positive field and a positive charge will induce a negative field in the surroundings.

As additional charge edq is introduced to the site of interest the energy will change according to

$$dE = \Phi_q e \, dq \quad (1.7)$$

The energy I required to remove an electron can be found by integrating Eqn. 1.7 from q to $q + 1$

$$I = \int_q^{q+1} \Phi_q e \, dq \quad (1.8)$$

where I is the ionization energy. Eqns. 1.6 - 1.8 apply only to a localized charge q . The ionization energy I in this case refers to the ionization energy of a core electron rather than a valence electron, because a core electron is more localized than a valence electron. Performing the integration in Eqn. 1.8 leads to

$$I = \Phi_q e - \alpha' e^2 / 2 \quad (1.9)$$

$\Phi_q e$ is the potential energy of an electron arising from the ground-state charge distribution. This was defined in section 1.2 as the initial-state effect V . $\alpha' e^2 / 2$ is the polarization/relaxation in the surroundings due to the introduced charge, defined in

section 1.2 as the final-state effect R . Substituting $\Phi_q e = V$ and $\alpha' e^2/2 = R$ into Eqn. 1.9 gives the following expression for the ionization energy I :

$$I = V - R \quad (1.10)$$

We now have an expression relating V and R and might expect a relation between Eqn. 1.10 and the electronegativity χ . Measured ionization energies are often not quoted as absolute values because of differences in calibration scales, but rather as shifts in ionization energies relative to some standard. Eqn. 1.10 can then be written as

$$\Delta I = \Delta V - \Delta R \quad (1.11)$$

where the ionization, potential, and relaxation energies are now expressed as shifts relative to the reference compound. Thomas⁹ showed a linear relationship between shifts in carbon 1s ionization energies and substituent electronegativities for halogenated methanes. It is this linear relationship which has allowed the use of XPS to determine the electronegativity of the $-\text{CF}_3\text{SO}_2$, $-\text{SF}_5$, and $-\text{SO}_2\text{F}$ groups.

2. EXPERIMENTAL PROCEDURES AND DATA ANALYSIS

2.1 The Spectrometer

All measurements were made using the Oregon State University cylindrical mirror electron spectrometer¹⁰. A cross section view is shown in Figure 2.1¹¹. The three main components of the spectrometer are the x-ray source, the cylindrical mirror electron energy analyzer, and the detector.

2.1.1 The X-ray Source

Aluminum $K\alpha$ x-rays were used to determine the C1s and S2p ionization energies. The $K\alpha$ x-rays were generated by bombarding a hollow aluminum anode with electrons generated from a thoriated tungsten filament. The generation of $K\alpha$ x-rays first requires the ionization of an aluminum 1s electron. The excited atom then emits a $K\alpha$ x-ray when a 2p electron fills the 1s vacancy. A voltage of about 9kV was applied to the anode while the filament was heated to produce an emission current of about 50 milliamperes. Because some of the incident electrons result in heating the anode rather than producing $K\alpha$ x-rays, it is necessary to cool the anode with running water.

The x-ray tube and gas cell are shown in Figure 2.2. The filament encircles the anode as shown in Figure 2.2¹¹. A drawback of this design is that the filament can flex and ground out. In an attempt to reduce the time spent adjusting the filament, a macor ceramic bead was placed over the portion of the filament farthest from the filament posts, as shown in Figure 2.2. This addition did help in preventing the filament from grounding and had no apparent detrimental effects. The macor bead was in place for measurement

of the following compounds: CF_3SSCF_3 , $\text{SF}_5\text{CH}_2\text{CH}_2\text{Br}$, $\text{SF}_5\text{CF}_2\text{SO}_2\text{F}$, $(\text{CF}_3\text{SO}_2)_2\text{CF}_2$, $\text{SF}_5\text{CH}=\text{CH}_2$, $\text{CF}_2\text{HSO}_2\text{F}$, and $\text{SF}_5\text{CH}_2\text{CH}_3$.

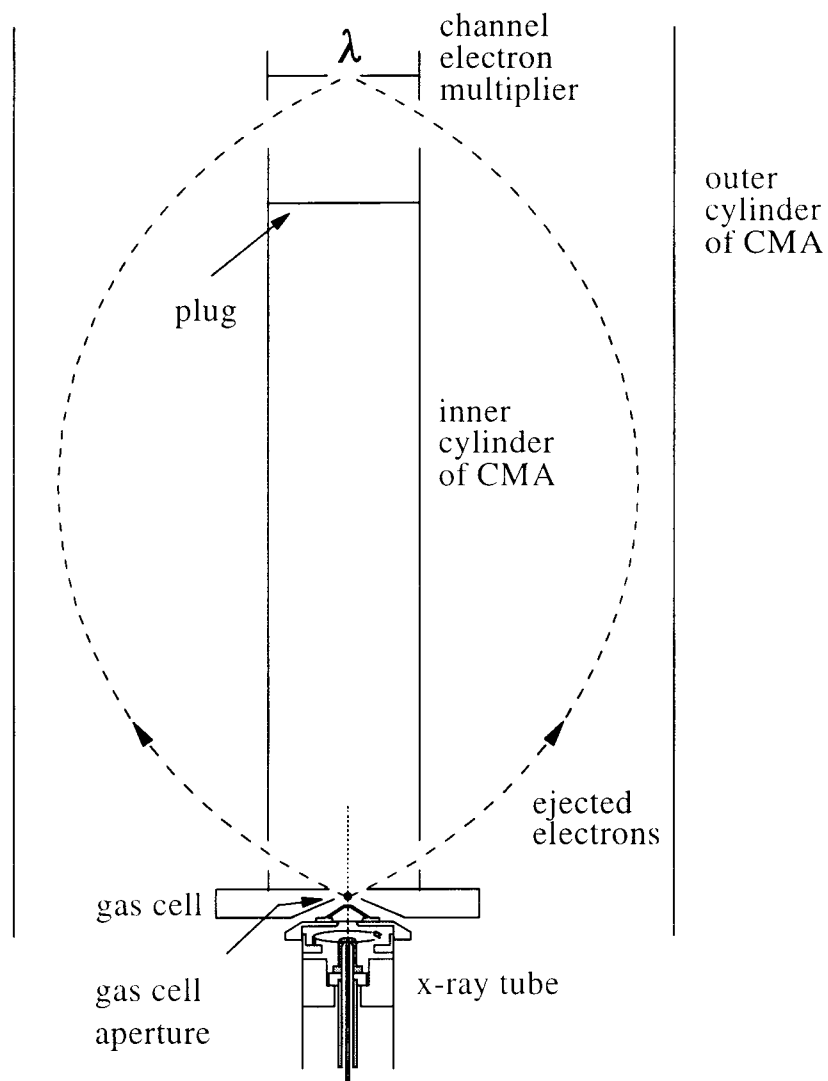


Figure 2.1: Cross section view of Oregon State University spectrometer main components.

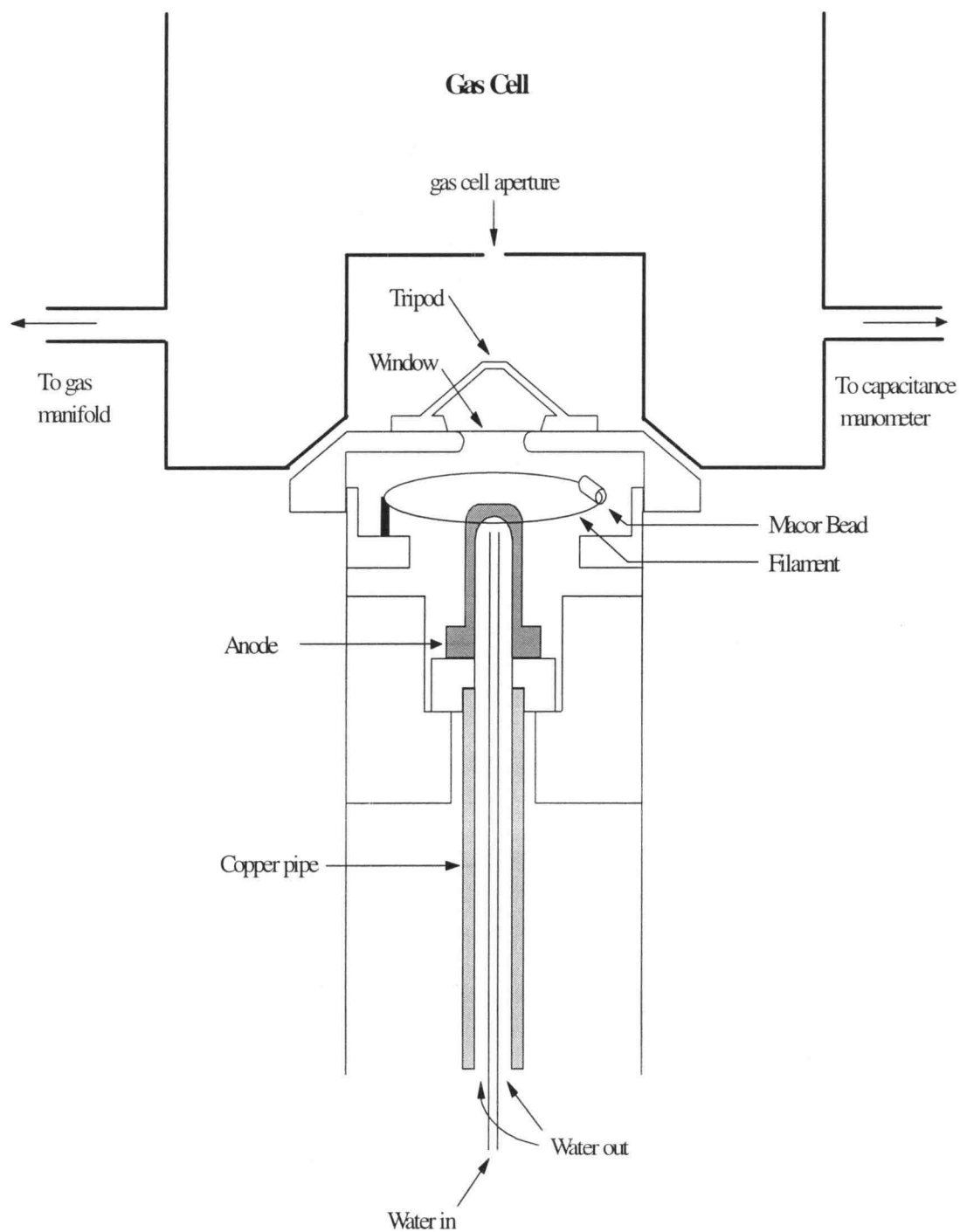


Figure 2.2: Cross section view of gas cell and major x-ray tube components.

The x-ray tube is isolated from the gas cell with a 1.5-micron thick plastic window. The plastic window has an aluminum coating to provide conductivity and is sprayed with graphite on the side facing the spectrometer to prevent surface charging. The aluminum $K\alpha$ x-rays (1486.553 ± 0.010 eV)¹² pass through this window and ionize the gaseous sample within the gas cell. A tripod shield was placed above the x-ray window to minimize background carbon 1s electrons arising from x-rays striking the edges of the graphite-coated gas cell aperture, although these background electrons were not completely eliminated, as can be seen in Figure 2.3. The electrons ejected from the gaseous sample then enter the cylindrical mirror energy analyzer.

The spectrometer is equipped with a safety system that will shut off the high voltage power supply to the x-ray tube if any of the following criteria are not met: cooling water must be supplied to the x-ray cooling ring and anode, the spectrometer must have a vacuum of about 10^{-6} torr, the high voltage safety relay box must be closed, and the door under the spectrometer must be closed to prevent access to the x-ray high voltage lead.

The pressure in the x-ray tube and the tank of the spectrometer are measured with a thermionic gauge. The thermionic gauge first generates electrons by heating a filament. These electrons then bombard gas molecules present and the resulting positive ion current is measured¹³. The gas cell is equipped with a capacitance manometer to read gas pressures in the gas cell while a spectrum is being measured. The tank of the spectrometer and the x-ray tube are pumped individually with diffusion pumps. It was not necessary to use liquid nitrogen in the cold finger to lower the pressure for these experiments.

2.1.2 The Cylindrical Mirror Analyzer

The cylindrical mirror analyzer (CMA) consists of two coaxial cylinders.

Electrons enter the inner cylinder from the gas cell and those traveling at the proper angle exit through a slit in the bottom of the inner cylinder. Electrons having a kinetic energy matched to the focusing voltage applied to the outer cylinder are focused through slits on the top of the inner cylinder onto the detector. A plug in the top of the inner cylinder prevents electrons from reaching the detector without first being focused through the outer cylinder, as is shown in Figure 2.2.

Fringe effects are essentially eliminated by 11 concentric copper rings placed at the top and bottom of the cylinders. A voltage is applied to each ring equal to the voltage that an infinitely long cylinder would have at that position in the spectrometer. The spectrometer is surrounded with 2 concentric sheets of mumetal to minimize the effects of external magnetic fields. The mumetal is degaussed by passing an alternating current slowly raised to 10A and decreased to 0A through copper wires coiled between the inner and outer mumetal sheets.

2.1.3 The Detector

A channel electron multiplier detector (channeltron) is placed on the common axis of the cylinders. The channeltron has one continuous glass dynode with a semiconducting inner surface. A potential of 2300V was applied across the channeltron, resulting in a gain of approximately 10^8 .¹⁴

2.1.4 Electronics and Computer

A PC has replaced the DEC 11/23 microcomputer described by Haak¹⁵ et al.; the PC is central to the high-voltage scanning system and detector electronics. The PC controls two 10 V digital-to-analog converters coupled to a 5 kV operational amplifier such that one converter has a gain of 500 and the other has a gain of 40. Optical isolators connect the converters to the computer in order to prevent computer noise from reaching the operational amplifier. The high-gain system allows a pedestal voltage between 0 and 5000 V to be selected in steps of 0.3V and the low-gain system allows the voltage to be swept in steps of 0.025 V over a 400 V range. The PC also controls the scan over a selected voltage range with a selected time interval per step.

The detector output connects to a preamplifier which converts the electron pulse to a voltage and then amplifies this voltage. The preamplifier connects to a constant fraction discriminator which selects pulses above a certain height and sends this signal to the computer.

2.2 Measuring a Spectrum

Spectra were obtained over two different time periods. The first set was collected intermittently between February and December 1997, while the second set was obtained between July and December 1998.

All samples analyzed were liquids at room temperature with the exception of SF₅Br gas; they were prepared in the laboratory of Gary L. Gard.¹⁶ Most samples were held in glass ampules and were attached directly to stainless steel needle valves on the gas manifold. SF₅Br was held in a small gas cylinder and attached directly to the gas

manifold. The gas manifold is connected to the gas cell with stainless steel tubing, and the gas cell is located directly above the x-ray tube as shown in Figure 2.1. With too high pressure in the gas cell counting efficiencies decrease, and with excessively high pressure the x-ray window can break. SF_5CF_3 is a liquid at room temperature with such a high vapor pressure that the gas manifold needle valve was insufficient to regulate the gas flow within a proper range. Approximately 6 feet of coiled copper tubing was added between the sample container and the needle valve. The copper tubing served as a reservoir into which a small amount of SF_5CF_3 was expanded, resulting in a lower pressure presented to the needle valve.

It is necessary to calibrate the energy scale for each measured spectrum, as described in section 2.3.2. For this purpose neon was mixed with the sample and neon 1s and neon 2s energies were measured with each spectrum. Their known ionization energies were used in calibrating the energy scale. The sample and neon calibration gases were each kept at a pressure of about 0.02 torr.

The program PESCADI6 was used to control the analyzer and collect the data. The operator specifies the low voltage setting, the number of channels, the voltage increment per channel, and the time spent counting each channel. Four different voltage ranges were scanned for these experiments to determine positions of the carbon 1s, sulfur 2p, neon 1s and neon 2s ionization peaks in the spectrum. Typically 81 to 121 channels were scanned in each region, with a voltage increment of 0.1 volts per channel. Each region was scanned sequentially until approximately 1000 counts were obtained at the peak maxima. Two to four spectra were obtained for each compound. Only one spectrum was obtained for CF_3SSCF_3 . The $\text{SF}_5\text{CH}_2\text{CH}_3$ C 1s and S 2p spectra are shown

in Figure 2.3 with the Ne 1s and Ne 2s spectra taken simultaneously with the sample spectra. The solid line in the C 1s spectrum is the non-linear least squares fit generated using Igor Pro as described in section 2.3.1. The peak at approximately channel 63 (966 V) is the C 1s background peak as mentioned in section 2.1.1. The asymmetry of the S2p spectrum arises from the spin-orbit splitting (1.2eV) of the orbital.

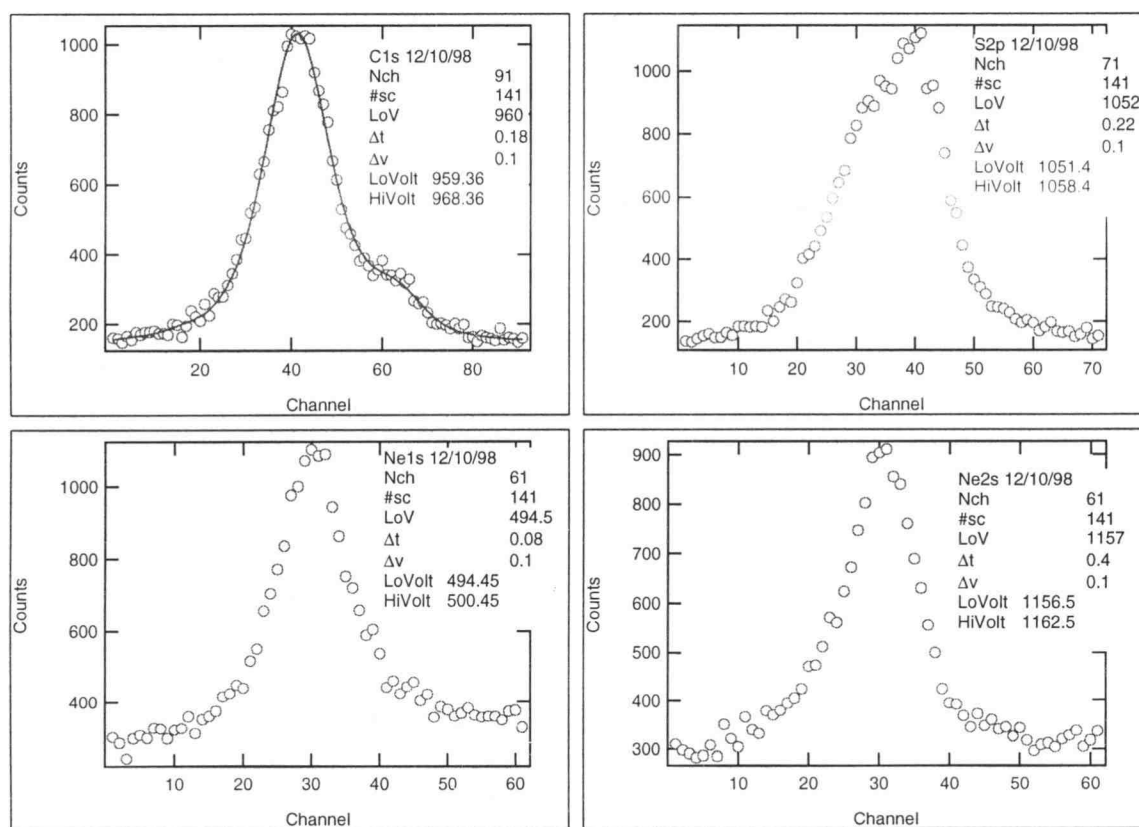


Figure 2.3: $\text{SF}_5\text{CH}_2\text{CH}_3$ C 1s and S 2p spectra with the simultaneously measured Ne 1s and Ne 2s spectra. The solid line in the C 1s spectrum is the non-linear least squares fit generated with Igor Pro. The C 1s background peak is seen at approximately channel 63.

2.3 Data Analysis

2.3.1 Determining Peak Positions

Peak positions were calculated using the LSMV program written by T.X. Carroll. The LSMV program uses non-linear least squares methods to fit a Voigt function with a linear background included. The Voigt function given by Eqn. 2.1 is a convolution of Gaussian and Lorentzian distributions:

$$V(A, x_0, \Gamma_G, \Gamma_L, x) = A \int_{-\infty}^{\infty} \frac{e^{-\frac{(x-x')^2}{\Gamma_G^2}}}{(x'-x_0)^2 + \frac{\Gamma_L^2}{4}} dx' \quad (2.1)$$

where A is the amplitude, x_0 is the peak position, and Γ_G and Γ_L are the gaussian and lorentzian peak widths respectively. LSMV varies A, x_0 , Γ_G and Γ_L until the best fit is achieved. The Gaussian contribution to the peak shape originates from the instrumental resolution and the Lorentzian contribution originates from the lifetime of the excited state.

For several of the compounds studied the carbon 1s peak was separated from the carbon 1s background peak by only ten to twenty channels. LSMV was unable to correctly determine the sample carbon 1s peak position in these cases, and Igor Pro was used to determine these peak positions. After the sample spectrum was completed all gases were turned off and the carbon 1s background spectrum was taken. Using an Igor Pro fitting routine designed by T.X. Carroll, this experimental background spectrum was included as part of the non-linear least squares fitting function.

2.3.2 Calibration

Ionization energies (IE) can be determined from the energy of the incident photon ($h\nu$), the kinetic energy of the ejected electron (K), and the recoil energy of the remaining ion (R) using Eqn. 2.2:

$$IE = h\nu - K - R \quad (2.2)$$

Determination of the kinetic energy of the photoelectron will be discussed first.

The photoelectron kinetic energy can be determined from Eqn. 2.3:

$$V = CK + B \quad (2.3)$$

where V is the focusing voltage (in V), K is the kinetic energy (in eV), B is the offset voltage, and C is the spectrometer constant. The offset voltage results from positive ions and surface-charging within the gas cell. Both B and C vary slightly over time and must be determined with each experiment. As mentioned in section 2.2 neon was measured in conjunction with the sample for each experiment. The neon 1s ionization energy (870.273 ± 0.014 eV) determined by Saethre et. al.¹⁷, the neon 2s ionization energy (48.476 ± 0.002 eV) known from optical spectroscopy^{18,19}, and the recoil energies calculated from conservation of momentum equations were used to calculate the kinetic energies using Eqn. 2.2. A plot of the focusing voltage versus kinetic energy for both the neon 1s and 2s data points, as shown in Figure 2.4, allows B and C to be calculated for each measured spectrum.

Once the constants B and C are determined for each spectrum, Eqn. 2.3 can be used to calculate the kinetic energy of the sample C1s and S2p photoelectrons. With these kinetic energies and the calculated recoil energies for the sample molecule, Eqn. 2.2 is used to determine the C1s and S2p ionization energies.

In reality the plot shown in Figure 2.4 is not linear, with deviations from linearity arising from relativistic effects.²⁰ The program CALBTN²¹ takes as input the positions of the peaks in the spectrum for the sample under investigation and the neon calibration as well as the masses of the molecules involved. It makes the necessary recoil and relativistic corrections and returns values of the desired ionization energies as well as the constants C and B.

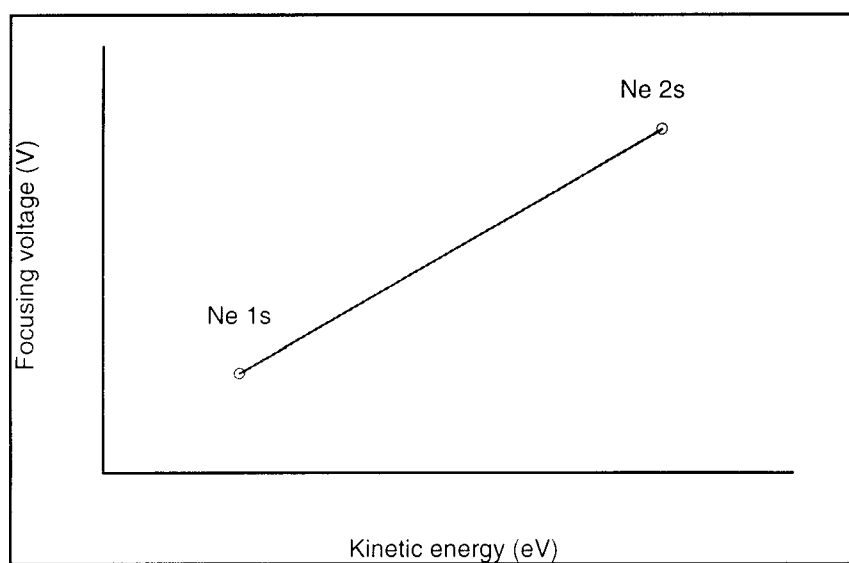


Figure 2.4: Plot of Ne 1s and Ne 2s calibrants from which B and C can be calculated for each spectrum.

3. RESULTS AND DISCUSSION

3.1 Electronegativities of $-\text{SF}_5$, $-\text{CF}_3\text{SO}_2$, and $-\text{SO}_2\text{F}$

The C 1s and S 2p core-ionization energies measured for the 17 compounds of this work are listed in Table 1 of the Appendix. Also included is the Br 3d core-ionization energy measured for SF_5Br . The C 1s data for 7 of these compounds were used in determining the electronegativity of the $-\text{SF}_5$, $-\text{CF}_3\text{SO}_2$, and $-\text{SO}_2\text{F}$ groups. The XPS C 1s core-ionization energies reported by Jolly et al.²² for 27 other compounds were also used in determining the group electronegativities. The ionization energies for all the compounds used in calculating the $-\text{SF}_5$, $-\text{CF}_3\text{SO}_2$, and $-\text{SO}_2\text{F}$ group electronegativities are shown in Table 2 of the Appendix, with the seven values measured in this work listed first. Electronegativities for $-\text{CH}_3$, $-\text{CF}_3$, $-\text{Cl}$, and $-\text{Br}$ substituents were also calculated from the experimental data to provide comparison with previously measured values.

In order to calculate the group electronegativities each compound was viewed as consisting of a central carbon atom attached to different substituents. The substituents considered were $-\text{F}$, $-\text{Cl}$, $-\text{Br}$, $-\text{CH}_3$, $-\text{CF}_3$, $-\text{SF}_5$, $-\text{CF}_3\text{SO}_2$, and $-\text{SO}_2\text{F}$. For example, CH_3CH_3 consists of a central carbon atom with one $-\text{CH}_3$ group and 3 hydrogen atoms attached. If we consider ionization energies relative to that of CH_4 , then the hydrogen substituents can be ignored. Labeling the central carbon with an asterisk, $\text{CF}_3\text{C}^*\text{F}_2\text{CF}_3$ consists of two $-\text{CF}_3$ groups and two $-\text{F}$ substituents. The substituents for each of the 34 compounds used to calculate electronegativities are summarized in Table 2 of the Appendix.

Shifts in the ionization energies relative to methane were calculated and equations in the form of Eqn. 3.1 were solved:

$$I_{C_{WXYZ}} - I_{CH_4} = c_w n_w + c_x n_x + c_y n_y + c_z n_z \quad (3.1)$$

where $I_{C_{WXYZ}}$ is the central carbon 1s ionization energy of the compound of interest. n_w , n_x , n_y , and n_z are the number of each substituent attached to the central carbon atom, and c_w , c_x , c_y , and c_z are the coefficients to be solved for. As mentioned earlier, hydrogen substituents were given a coefficient of zero. Linear regression between the ionization energy shifts and the values of n was used to give coefficients for each of the substituents: -F, -Cl, -Br, -CH₃, -CF₃, -SF₅, -CF₃SO₂, and -SO₂F.

With the coefficients determined, Eqn. 3.2 was used to calculate the core-ionization energy shifts.

$$\chi_j = \chi_H + \frac{c_x (\chi_F - \chi_H)}{c_F} \quad (3.2)$$

These calculated values are included in Table 2 of the Appendix. The calculated core-ionization energy shifts are plotted against the experimental values in Figure 3.1. The linear regression fit line is also included in the plot. There is excellent agreement between the core-ionization energy shifts calculated using Eqn. 3.2 and experimental values, with a linear regression correlation coefficient of 0.99, an intercept of -0.11, and a slope of 1.01 for the least squares fit line. This comparison shows that the measured ionization energies are well represented by Eqn. 3.1.

Using known electronegativity values for H and F of 2.2 and 3.98²³ respectively

and coefficients of zero for H and 2.65 for F, a scale was generated from which electronegativity values for the remaining substituents were calculated. This is shown graphically in Figure 3.2 and numerically with Eqn. 3.2.

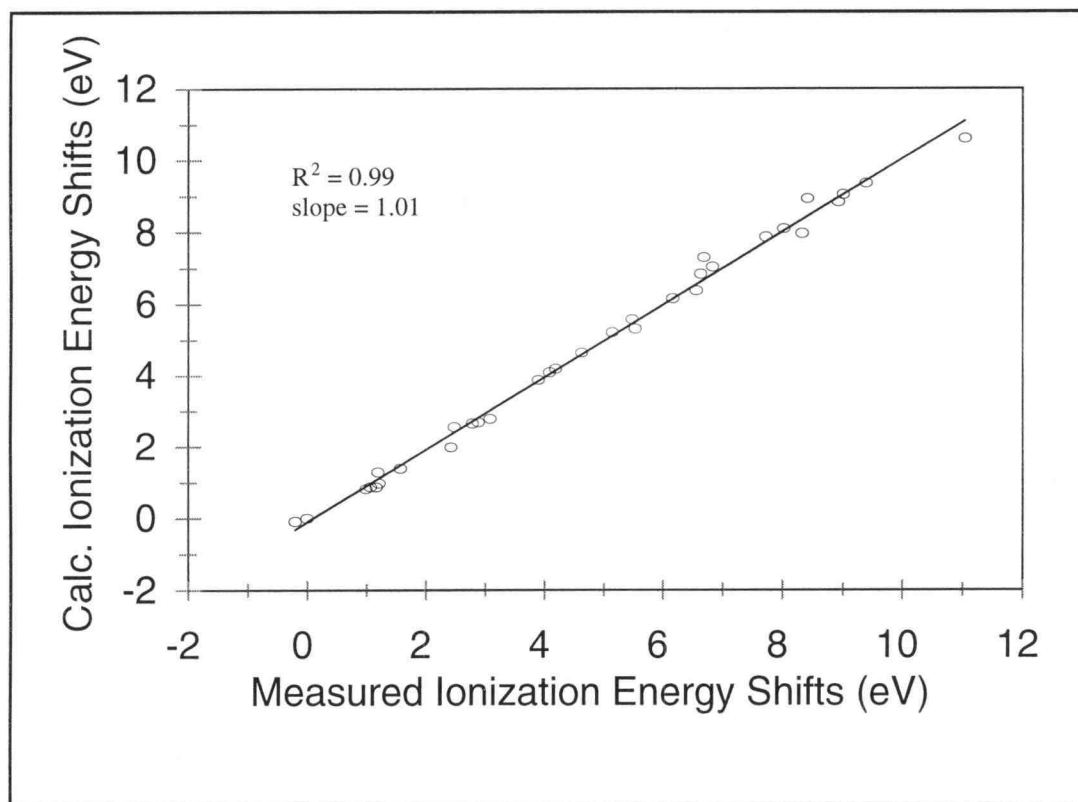


Figure 3.1: Plot of core-ionization energy shifts calculated using Eqn. 3.1 versus measured core-ionization energies. The solid line is the least squares fit to the data.

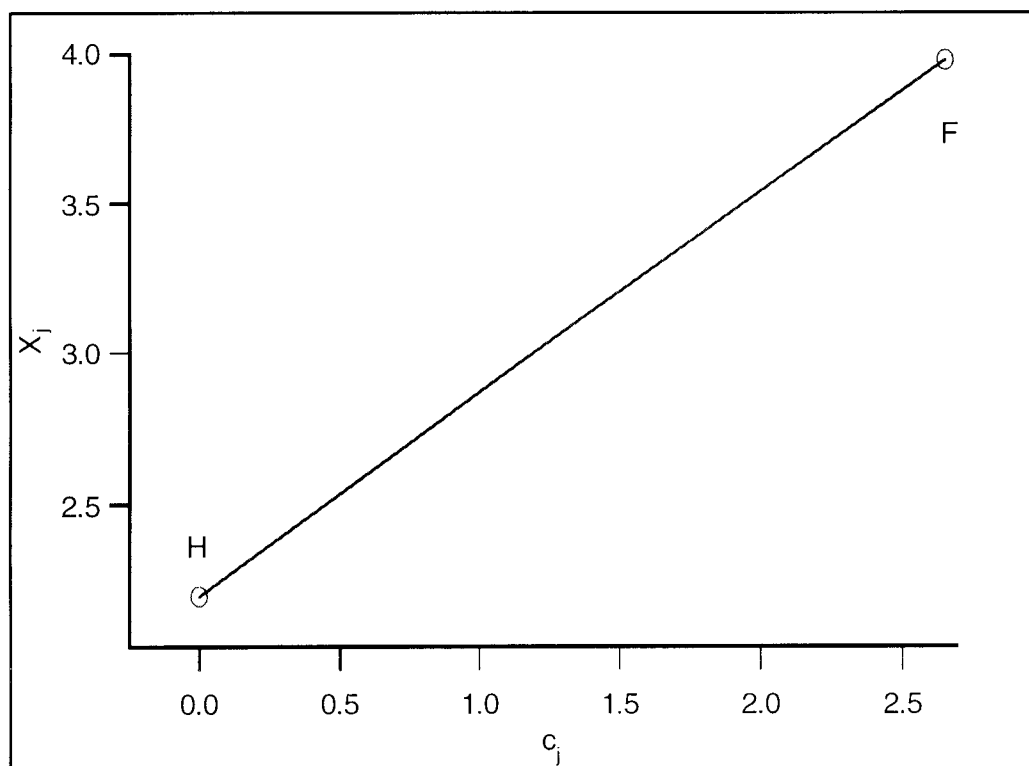


Figure 3.2: Graphic representation of Eqn. 3.2 used to calculate electronegativities (χ_i) from c coefficients (c_i).

The experimental electronegativities calculated from Eqn. 3.2 are shown in Table 3.1 and are compared with other experimental values. No other experimental values were found for $-\text{CF}_3\text{SO}_2$ and $-\text{SO}_2\text{F}$.

Table 3.1: Experimental electronegativities (Pauling units).

	Experimental (current)	Experimental (other)
-Cl	3.14 ± 0.02	$2.83 - 3.16^a$
-Br	2.85 ± 0.04	$2.74 - 2.96^a$
$-\text{CH}_3$	2.14 ± 0.06	2.3^b
$-\text{CF}_3$	2.78 ± 0.08	$3.35^b, 3.3^c$
$-\text{SF}_5$	2.81 ± 0.12	$2.8^d, 3.1^e$
$-\text{CF}_3\text{SO}_2$	2.49 ± 0.09	
$-\text{SO}_2\text{F}$	2.92 ± 0.12	

^aCotton et al.²³

^bWells²⁴, from vibrational data.

^cBell et al.²⁵, from IR absorption wavelength of P=O bond.

^dBoden et al.²⁶, from NMR J_{HH} coupling constants.

^eCanselier et al.²⁷, from ^{13}C -NMR chemical shifts.

The electronegativity of -Br and -Cl are in agreement with accepted values. However, the electronegativity of $-\text{CH}_3$ is somewhat lower than accepted values and $-\text{CF}_3$ is most notably lower than other experimental values. The only other experimental electronegativities found for $-\text{CF}_3$ and $-\text{SF}_5$ are listed in Table 3.1. It must be noted that the experimental electronegativities of $-\text{SF}_5$ found here and by other authors^{26,27} are in large disagreement with theoretical values calculated through various methods.

The currently measured group electronegativities listed in Table 3.1 are compared with theoretical values in Table 3.2. The methods of Bratsch²⁸, Huheey²⁹, and Carver³⁰ are all based on the Principle of Electronegativity Equalization proposed by Sanderson³¹. Bratsch²⁸ calculated group electronegativities with Eqn. 3.3:

$$\chi_G = \frac{N_G}{\sum \frac{v}{\chi}} \quad (3.3)$$

where χ_G is the group electronegativity, N_G is the total number of atoms in the group, v is the number of atoms of a particular element, and χ is the Pauling electronegativity of that element. Huheey²⁹ used the orbital electronegativities of Hinze et al.³² to calculate electronegativities. Carver³⁰ proposed a Modified Sanderson method based on stability ratios (as described in Section 3.3) to calculate electronegativities.

Table 3.2: Experimental electronegativities compared with calculated values (Pauling units).

	Expt.	Electronegativity Equalization (EE)			No EE	
		Huheey ^a	Carver ^b	Bratsch ^c	Thomas ^d	Constantinides ^e
-CH ₃	2.14	2.27	2.34		1.54	1.57
-CF ₃	2.78	3.46	3.45	3.49	1.83	2.8
-SF ₅	2.81	3.70 ^f	3.66	3.65	2.51	
-CF ₃ SO ₂	2.49	3.76 ^g	3.40	3.31	2.00	
-SO ₂ F	2.92	4.08 ^g	3.34	3.28	2.30	

^abased on orbital electronegativities; ^bModified Sanderson method³⁰; ^cbased on Bratsch's definition;

^dMulliken ; ^ebased on Pauling method with geometric mean; ^fcalculated by this author using S octahedral valence state; ^gcalculated by this author using S sp³ valence state.

Sanderson describes the Principle of Electronegativity Equalization as follows:

“When two or more atoms initially different in electronegativity combine, they adjust to the same intermediate electronegativity in the compound.”³⁰ The atom of greater

electronegativity will accumulate more electrons, increasing the partial negative charge and decreasing the electronegativity on that atom in the molecule. The atom of lesser electronegativity will lose electrons, increasing the partial positive charge and increasing the electronegativity on that atom in the molecule.

Most theoretical calculations of electronegativity have been based on this principle. Huheey³³ noted that the relationship between polar substituent constants and group electronegativities was best predicted by assuming 80% electronegativity equalization rather than 100% equalization. From this, one may question the validity of the Principle of Electronegativity Equalization.

Included in Table 3.2 are electronegativities calculated by Thomas et al.³⁴ Thomas used MP2/6-31G++** calculations to determine the ionization energy and electron affinity for the group of interest. The Mulliken definition of electronegativity as given in Eqn. 1.4, $\chi^M = (IE + EA)/2$, was then used to calculate the group electronegativity. The assumption of electronegativity equalization was not necessary in these calculations.

Constantinides³⁵ calculated the electronegativity of the $-CH_3$ and $-CF_3$ groups using a variation of Pauling's thermochemical method based on the geometric mean. The formula he proposed is given by Eqn. 3.4:

$$\chi_R = \chi_H \pm 0.183 \{ D(R-H) - [D(R-R) \cdot D(H-H)]^{1/2} \}^{1/2} \quad (3.4)$$

Appropriate thermochemical data could not be located to calculate the electronegativities of the other groups studied here. As noted by Wells²⁴, the electronegativity calculated from empirical data is entirely dependent on the approach used. Wells²⁴ lists electronegativities of 2.2 - 2.4 for $-CH_3$ and 2.86 for $-CF_3$ using modifications of Eqn. 3.4.

It therefore seems possible to obtain almost any value by simply defining a particular equation for combining thermochemical data.

The trends in the currently measured electronegativities listed in Table 3.1 are not easily understood. The value for -Cl is too high, -CH₃ is slightly low, -CF₃ is very low, and -SF₅ is in agreement with other experimental values found but significantly lower than theoretical values. There is also disagreement on the relative relationship between the electronegativities of -CF₃ and -SF₅ found in the literature, some authors concluding that $\chi_{\text{CF}_3} > \chi_{\text{SF}_5}$ and other authors concluding that $\chi_{\text{CF}_3} < \chi_{\text{SF}_5}$. Kimura et al.³⁶ conclude from UV absorption data for saturated organic iodides and bromides that $\chi_{\text{CF}_3} > \chi_{\text{SF}_5}$; Brant et al.³⁷ conclude from XPS data for substituted acetylenes that $\chi_{\text{CF}_3} > \chi_{\text{SF}_5}$; Sheppard³⁸ concludes from ionization constants for substituted benzoic acids that $\chi_{\text{CF}_3} < \chi_{\text{SF}_5}$; and Thrasher et al.³⁹ conclude from ¹H chemical shifts of *N*-methylamines that $\chi_{\text{CF}_3} < \chi_{\text{SF}_5}$.

In order to determine if relaxation effects were lowering ionization energies and giving low electronegativities in the current work, Thomas⁴⁰ compared measured ionization energies with energies calculated from the equivalent cores method and Koopmans' theorem. The plot is shown in Figure 3.3. Core ionization energies are calculated with the equivalent cores method by first calculating the total energy of the molecule of interest, and then the total energy of the molecule with the core-ionized atom replaced with a positive ion of the $Z + 1$ element. For example, the core ionization energy for CH₄ can be determined by calculating the total energy of CH₄ and then the total energy of N⁺H₄. The shift in core ionization energy can then be determined relative to some reference compound. Equivalent cores ionization energies thus include

relaxation effects. Using Koopmans' theorem one simply takes the negative of the neutral molecule orbital energy as the ionization energy, so no relaxation effects are

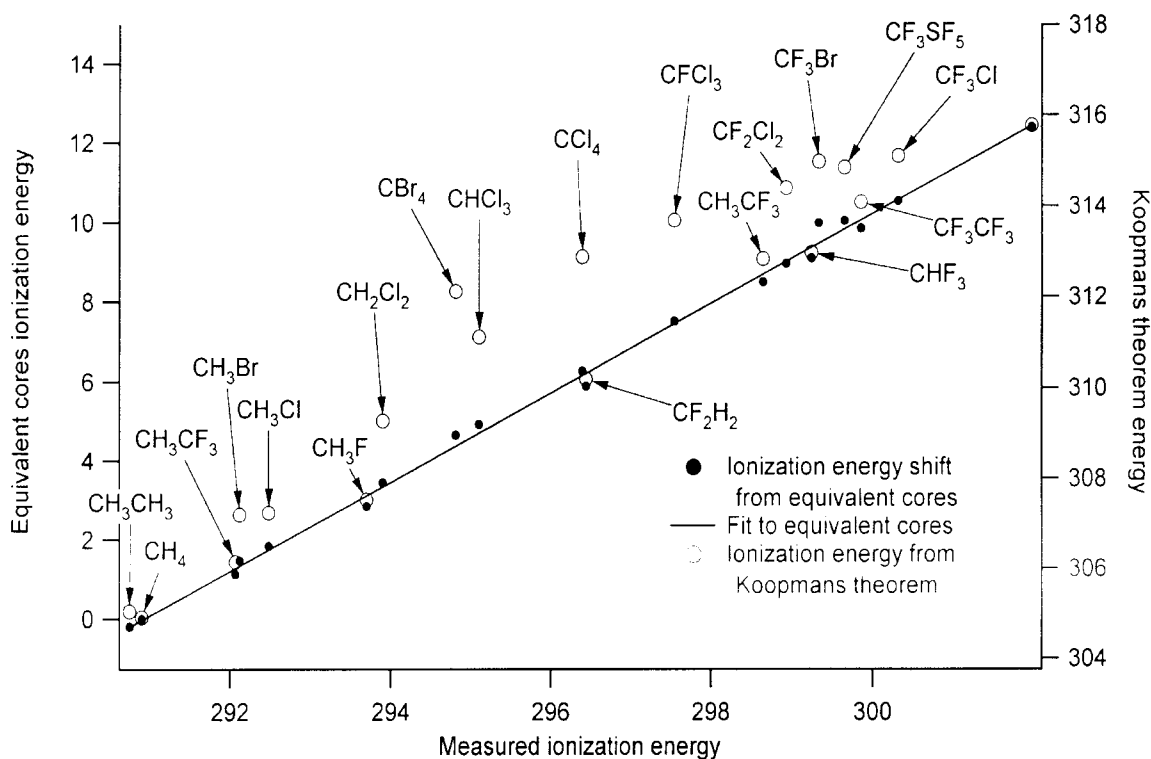


Figure 3.3: Plot of measured ionization energies against Equivalent cores and Koopmans' theorem energies.⁴⁰

included in the ionization energy. These results suggest a small relaxation energy for -CH₃ and -CF₃ and a large relaxation energy for -Cl. The low electronegativity value currently measured for -CF₃ most likely does not result from relaxation effects. The relaxation energy of -SF₅ appears to be quite significant, but not larger than that of -Cl or -Br. We therefore might expect the electronegativity of -SF₅ measured with XPS to be lower than values measured with a method not involving ionization with accompanying relaxation effects. Our experimental value for χ_{SF_5} is in agreement with experimental

values measured through NMR chemical shifts, and our value for χ_{CF_3} is significantly lower than values measured through vibrational data.

3.2 Comparison of $-\text{SF}_5$ Electronegativity from C 1s and S 2p Data

The electronegativity of the $-\text{SF}_5$ group was calculated from C 1s data as described in section 3.1; it was also calculated from S 2p data using molecules of the form SF_5X , where the X group was F, Cl, Br, and $-\text{SF}_5$. The S 2p ionization energies for SF_6 (reported by Jolly²² et al.), SF_5Cl (measured by Asplund⁴¹ et al.), and the currently measured SF_5Br S2p ionization energy were plotted against known²³ electronegativities of the halogens F, Cl, and Br. The S 2p ionization energy currently measured for SF_5SF_5 was then used to determine the $-\text{SF}_5$ electronegativity from the plot. The data used to generate the plot are shown in Table 3.3. The electronegativities of F, Cl, and Br and the S 2p ionization energies were calculated using the slope and y-intercept of the least squares fit line. These values are included in Table 3.3 for comparison with their known values. The plot of S 2p ionization energies versus electronegativity of X is shown in Figure 3.4. The solid line in Figure 3.4 is the least squares fit line for the three data points. The correlation coefficient is 0.989 and the slope of the least squares fit line is 1.29.

The electronegativity of $-\text{SF}_5$ calculated from C 1s ionization energies as described in section 3.1 is 2.81 ± 0.12 ; the value calculated from S 2p ionization energies is 2.79 ± 0.13 .

3.3 Correlation with modified Sanderson Calculations

Sanderson made the proposal that the electronegativity of an atom “is roughly proportional to the average electronic density and is measured by the stability ratio.”⁴²

Table 3.3: SF_5X S 2p ionization energies and halogen electronegativities (χ) used to calculate the electronegativity of $-\text{SF}_5$. Included for comparison with known values are the calculated electronegativities of F, Cl, and Br, and S 2p ionization energies for SF_5X , X = F, Cl, Br. (Electronegativities in Pauling units.)

X	SF_5X S 2p IE (eV)	χ	χ_{calc}	S 2p IE _{calc}
F	180.23	3.98	3.97	180.25
Cl	179.27	3.16	3.22	179.19
Br	178.87	2.96	2.91	178.93
SF_5	178.71		2.79 ± 0.13	

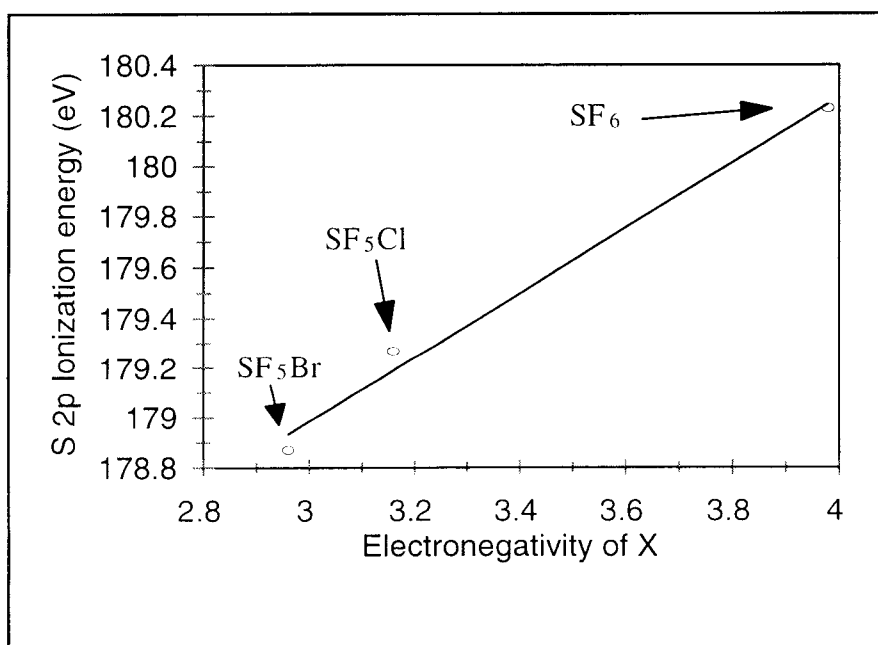


Figure 3.4: Sulfur 2p ionization energies versus electronegativity of group X. The line through the data is the least squares fit line.

The stability ratio (SR) is given by the ratio of the average electron density of the atom of interest (ED) to the electron density of an isoelectronic inert atom (ED_i), either real or hypothetical: $SR = ED/ED_i$. ED is the average number of electrons per \AA^3 and is given by $ED = Z/(4\pi r^3/3)$, where Z is the number of electrons on the atom and r is the covalent or ionic radius. For the isoelectronic inert atom r is determined by interpolating between real values. Sanderson used experimental atomic radii to calculate the stability ratios for many of the elements.⁴² Sanderson's proposal that stability ratios are related to electronegativity was based on the observation that atoms with a large ED (and therefore large SR) were the most electronegative elements and atoms with a small ED and SR were the least electronegative. Sanderson's SR and Pauling's electronegativity χ (derived from bond energies) are related by the equation⁴³ $\chi = (0.21SR + 0.77)^2$, which Sanderson used to support his connection between stability ratios and electronegativity.

Using the Principle of Electronegativity Equalization³¹ the SR for a molecule is given by the geometric mean of atomic stability ratios for all atoms in the molecule: $SR_M = (\prod_{i=1}^n SR_i)^{1/n}$ where n is the number of atoms and SR_i is the stability ratio for element i in the molecule. The partial charge δ on atom i is then found from the relation

$$\delta_i = (SR_M - SR_i)/\Delta SR_i \quad (3.5)$$

where ΔSR_i is a normalization factor given by $\Delta SR_i = 2.08(SR_i)^{1/2}$. The problems with this method of assigning partial charges to atoms in molecules are that atoms in different chemical environments within the molecule are given the same partial charges, and there is no distinction between structural isomers such as $\text{CH}_3\text{CH}_2\text{CH}_2\text{CH}_2\text{OH}$ and $\text{CH}_3\text{CH}_2\text{OCH}_2\text{CH}_3$.⁴⁴

Carver³⁰ et al. proposed a modified Sanderson method to avoid the problems of Sanderson's original method. In the modified Sanderson method the molecule is viewed as a collection of groups rather than a collection of atoms. The SR_M in Eqn. 3.5 becomes the group stability ratio (SR_G) in the modified Sanderson method, which accounts for different chemical environments within a molecule. The group stability ratio is calculated as the geometric mean of the stability ratio for the central atom of the group and the stability ratios of all subgroups attached to the central atom. The subgroups attached to the central atom of the group may be atoms or group, with each subgroup being broken down into atomic stability ratios. For example, SR_{CF_3} for the molecule CF_3SSCF_3 is found as follows:

$$SR_{CF_3} = (SR_C SR_F^3 SR_M')^{1/5} \quad SR_M' = (SR_S SR_M'')^{1/2} \quad SR_M'' = (SR_S SR_{CF_3}')^{1/2}$$

$$SR_{CF_3}' = (SR_C SR_F^3)$$

The overall expression for SR_{CF_3} is then given by the following:

$$SR_{CF_3} = (SR_C SR_F \{ SR_S [SR_S (SR_C SR_F^3)^{1/4}]^{1/2} \}^{1/2})^{1/5} \quad (3.6)$$

and the atomic charge on C in CF_3SSCF_3 can be found from Eqn. 3.7:

$$\delta_C = (SR_{CF_3} - SR_C) / \Delta SR_C \quad (3.7)$$

where $SR_C = 3.79$ as determined by Sanderson²² and $\Delta SR_C = 2.08(SR_C)^{1/2} = 4.05$.

Sastry⁴⁴ compared atomic charges calculated with Eqn. 3.7 to C1s ionization energy (IE) shifts. He reports a linear regression correlation coefficient of 0.95 between atomic charges calculated with Eqn. 3.7 and experimental C1s IE shifts. The atomic charges on carbon have been thus calculated for the compounds of this study to determine the correlation between the modified Sanderson method atomic charges and our experimental C1s IE shifts. The C1s IE of 290.8eV was used as the standard from which

the IE shifts were calculated. The calculated carbon atomic charges and the C1s IE shifts are shown in Table 3.3.

Sastry reports a least squares fit slope of 23.1, an intercept of 1.2, and $R^2 = 0.90$. This author obtained $R^2 = 0.87$, a slope of 23.1, and an intercept of 1.2 when fitting Sastry's reported data. Least squares analysis of the calculated atomic charge and currently measured C1s IE shifts gave $R^2 = 0.85$, a slope of 21.1, and an intercept of 0.7. Figure 3.5 shows the graph of calculated atomic charge versus the currently measured C1s IE for the compounds discussed here. The line through the data is the calculated atomic charges fit with Sastry's fit parameters. Data points significantly removed from the least squares fit line are numbered according to their index in Table 3.4.

As was observed by Sastry, the largest deviations from the least squares fit line result mostly from sp^2 hybridized carbons, although not all the sp^2 hybridized carbons show significant deviation. Sastry speculated that an improvement would be observed for sp^2 hybridized carbons if the final-state relaxation energy effects were included for delocalized π electrons. A following investigation by Patil⁴⁵ et al. provided additional support for this conclusion. The largest current deviations are seen for sp^3 hybridized $SF_5CF_2SO_2F$, both sp^2 hybridized carbons in $SF_5CF=CF_2$ and the sp^2 hybridized carbon SF_5CH- in $SF_5CH=CF_2$.

Table 3.4: Calculated atomic charges on carbon for gas phase molecules and the corresponding currently measured C1s IE shifts. An average atomic charge is reported for molecules in which C1s ionization energies were unresolved.

	Calculated atomic charge	Expt. C1s IE shift (eV)
1. SF ₅ CCH	-0.0292	0.91
2. SF ₅ CH ₂ CH ₃	0.0045	1.06
3. SF ₅ CH=CH ₂	0.0267	0.97
4. SF ₅ CH ₂ CH ₂ Br	0.0332	1.68
5. SF ₅ CH ₂ CH ₂ Cl	0.0434	1.73
6. SF ₅ CH ₂ SO ₂ F	0.1014	2.55
7. SF ₅ CH=CF ₂	0.1443	1.48
8. SF ₅ CH=CF ₂	0.2456	6.12
9. SF ₅ CFHSO ₂ F	0.2065	4.74
10. CF ₂ HSO ₂ F	0.2192	6.67
11. SF ₅ CF=CF ₂	0.2827	3.77
12. SF ₅ CF=CF ₂	0.2941	6.01
13. CF ₃ SSCF ₃	0.3002	7.50
14. CF ₂ (SO ₂ CF ₃) ₂	0.3086	8.50
15. SF ₅ CF ₂ SO ₂ F	0.3221	6.87
16. CF ₃ SO ₂ F	0.3362	9.13
17. SF ₅ CF ₃	0.3560	8.85

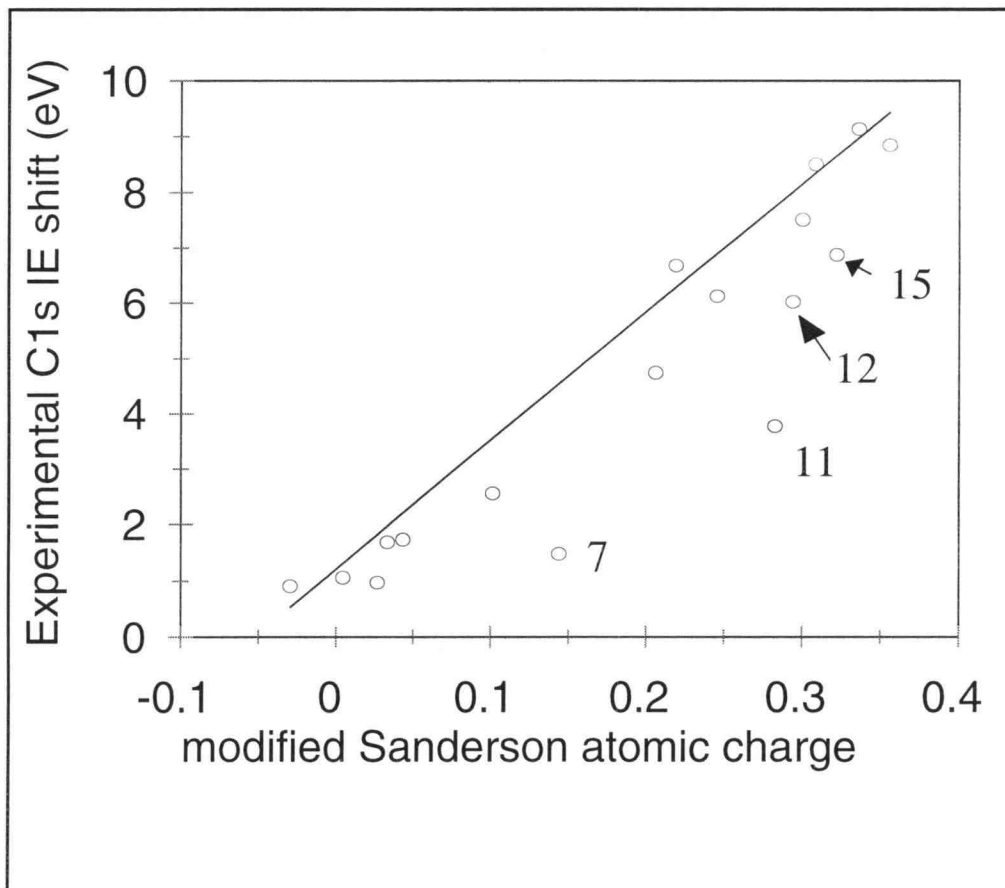


Figure 3.5: Plot of currently measured C1s IE shifts versus atomic charge calculated with modified Sanderson method. Sastry's least squares fit parameters were used to generate the line through the data. The numbers refer to compounds as indexed in Table 3.3.

4. CONCLUSIONS

The electronegativities of the substituents $-\text{SF}_5$, $-\text{CF}_3\text{SO}_2$, and $-\text{SO}_2\text{F}$ have been determined from this study to be 2.81 ± 0.12 , 2.49 ± 0.09 , and 2.92 ± 0.12 respectively. The electronegativities of $-\text{CF}_3\text{SO}_2$ and $-\text{SO}_2\text{F}$ appear to be the first reported, so no comparison can be made for these groups. The electronegativity of the $-\text{SF}_5$ substituent was determined from both C 1s ionization energies ($\chi_{\text{SF}_5} = 2.81 \pm 0.12$) and S 2p ionization energies ($\chi_{\text{SF}_5} = 2.79 \pm 0.13$); the values are in excellent agreement. These $-\text{SF}_5$ electronegativities agree with the only other numeric experimental values found, but are substantially less than the theoretical value of approximately 3.5 calculated using the Principle of Electronegativity Equalization^{29,30} and larger than the theoretical value of 2.51 calculated by Thomas³⁴ using the Mulliken definition of electronegativity.

The electronegativity currently measured for $-\text{CF}_3$ is 2.78 ± 0.08 , while other experimental values measured from vibrational data are 3.35^{24} and 3.3^{25} . As with $-\text{SF}_5$, the currently measured $-\text{CF}_3$ electronegativity is substantially less than the theoretical value of approximately 3.5 calculated using the Principle of Electronegativity Equalization^{29,30} and larger than the theoretical value of 1.83 calculated by Thomas.³⁴

There is disagreement in the literature^{36,37,38,39} on the relative magnitudes of χ_{SF_5} and χ_{CF_3} , some authors concluding $\chi_{\text{CF}_3} < \chi_{\text{SF}_5}$ and others concluding $\chi_{\text{CF}_3} > \chi_{\text{SF}_5}$. Not much insight seems to be gained through considering theoretical values. The validity of the Principle of Electronegativity Equalization is not certain, evidenced by Huheey's³³ conclusion that 80% Equalization improves the correlation between polar substituent constants and group electronegativities. The theoretical electronegativities based on

Electronegativity Equalization are all higher than the currently measured electronegativities, as shown in Table 3.2, and those calculated without Electronegativity Equalization are lower.

Finally, the Modified Sanderson method³⁰ gives a correlation of $R^2 = 0.85$ between atomic charges calculated with stability ratios and experimental C 1s ionization energy shifts. Electronegativities calculated with the Modified Sanderson method are based on the assumption of electronegativity equalization. As shown in Table 3.2 the electronegativities calculated with the Modified Sanderson method for $-\text{CH}_3$, $-\text{CF}_3$, $-\text{SF}_5$, $-\text{CF}_3\text{SO}_2$, and $-\text{SO}_2\text{F}$ are all significantly higher than the experimental values currently measured. For these groups, a correlation of $R^2 = 0.73$ is found between electronegativities calculated with the Modified Sanderson method and the experimental values. It is unclear why the currently measured experimental values are lower than theoretical values calculated with the assumption of electronegativity equalization.

REFERENCES

1. L.C. Pauling, "The Nature of the Chemical Bond", 2nd ed.; Cornell University Press: Ithaca, NY, 1948, p 58.
2. J. Mullay, from "Electronegativity", Springer-Verlag series on Structure and Bonding, Vol. 66, Editors K.D.Sen and C.K. Jørgensen, Springer-Verlag, Berlin Heidelberg, 1987, p 18.
3. L.C. Pauling, "The Nature of the Chemical Bond", 2nd ed.; Cornell University Press: Ithaca, NY, 1948, pp 47-60.
4. Ibid, p. 51-52.
5. R.S. Mulliken, *J. Chem. Phys.*, **2**, 1934, 782.
6. M.K. Kemp, "Physical Chemistry, A Step-by-Step Approach", vol. 6; Marcel Dekker, Inc.: New York, 1979, p 408.
7. E.J. Aitken, M.K. Bahl, K.D. Bomben, J.K. Gimzewski, G.S. Nolan, T.D. Thomas, *J. Am. Chem. Soc.*, **102**, 1980, 4873.
8. M.R. Siggel, T.D. Thomas, *J. Am. Chem. Soc.*, **108**, 1986, 4360.
9. T.D. Thomas, *J. Am. Chem. Soc.*, **92**, 1970, 4184.
10. P.H. Citrin, R.W. Shaw and T.D. Thomas, D.A. Shirley (Editor), "Electron Spectroscopy"; North-Holland Publishing Co.: Amsterdam, 1972, p 105.
11. Adapted with permission from M. Coville, "Inner-Shell Lifetimes of Small Gas-Phase Molecules", Ph.D. Dissertation, Oregon State University, 1996, pp 92-93.
12. E.G. Kessler, Jr., R.D. Deslattes, D. Girard, W. Schwitz, L. Jacobs and O. Renner, *Phys. Rev. A*, **6**, 1982, 2696.
13. D.P. Shoemaker, C.W. Garland and J.W. Nibler, "Experiments in Physical Chemistry", 6th ed.; McGraw-Hill Companies, Inc.: New York, 1996, p 634.
14. J.H. Moore, C.C. Davis, M.A. Coplan, "Building Scientific Apparatus, A Practical Guide to Design and Construction", Addison-Wesley Publishing Company: London, 1983, p 322.
15. H.W. Haak, G.A. Sawatzky, L. Ungier, J.K. Gimzewski, and T.D. Thomas, *Rev. Sci. Instrum.* **55** (5), 1984, 696.

16. G.L. Gard, Chemistry Department, Portland State University, P.O. Box 751, Portland, OR 97207-0751.
17. L.J. Saethre, T.D. Thomas and L. Ungier, *J. Electron Spectrosc. Relat. Phenom.*, **33**, 1984, 381-386.
18. J.A. Bearden, *Rev. Mod. Phys.*, **39**, 1967, 78.
19. J.C. Boyce, *Phys. Rev.*, **46**, 1934, 378.
20. T.D. Thomas, R.W. Shaw, Jr., *J. Electron Spectrosc. Relat. Phenom.*, **5**, 1974, 1081.
21. S.R. Smith, "Gas Phase X-ray Photoelectron Spectroscopy of Compounds Containing Multiple-Bonded Oxygen", Ph.D. Dissertation, Oregon State University, 1977, pp 34-40.
22. W.L. Jolly, K.D. Bomben, C.J. Eyermann, *Atomic Data and Nuclear Data Tables*, **31**, No. 3, 1984, 434.
23. F.A. Cotton, G. Wilkinson, "Advanced Inorganic Chemistry, a Comprehensive Text", 3rd edition, Interscience Publishers, New York, 1972, p 115.
24. P.R. Wells, "Progress in Physical Organic Chemistry", vol. 6: Interscience Publishers: New York, 1968, p 115.
25. J. Bell, J. Heisler, H. Tannenbaum, J. Goldenson, *J. Am. Chem. Soc.*, **76**, 1954, 5185.
26. N. Boden, J.W. Emsley, J. Feeney, L.H. Sutcliffe, *Trans Faraday Soc.*, **59**, 1963, 620.
27. J.P. Canselier, J.L. Boyer, V. Castro, G.L. Gard, J. Mohtasham, D.H. Peyton, F.E. Behr, *Magn. Res. In Chemistry*, **33**, 1995, 506.
28. S.G. Bratsch, *J. Chem. Educ.*, **62**, 1985, 101.
29. J.E. Huheey, *J. Phys. Chem.*, **69**, 1965, 3284.
30. J.C. Carver, R.C. Gray, D.M. Hercules, *J. Am. Chem. Soc.*, **96**, 1974, 6851.
31. R.T. Sanderson, "Chemical Periodicity", Reinhold Publishing Corporation, New York, 1960, p 37.
32. J. Hinze, H.H. Jaffé, *J. Am. Chem. Soc.*, **84**, 1962, 540.
33. J.E. Huheey, *J. Org. Chem.*, **31**, 1966, 2365.
34. T.D. Thomas, J. True, unpublished calculations.
35. E. Constantinides, *Proc. Chem. Soc.*, 1964, 290.

36. K. Kimura, S. Nagakura, *Spectrochimica Acta*, **17**, 1961, 166.
37. P. Brant, A.D. Berry, R.A. DeMarco, F.L. Carter, W.B. Fox, J.A. Hashmall, *J. Electron Spectrosc. Relat. Phenom.*, **22**, 1981, 119.
38. W.A. Sheppard, *J. Am. Chem. Soc.*, **84**, 1962, 3072.
39. J.S. Thrasher, J.B. Nielsen, *J. Am. Chem. Soc.*, **108**, 1986, 1108.
40. T.D. Thomas, unpublished.
41. L. Asplund, P. Kelfve, H. Siegbahn, O. Goscinski, H. Fellner-Feldegg, K. Hamrin, B. Blomster, K. Siegbahn, *Chem. Phys. Lett.*, **40**, 1976, 353.
42. R.T. Sanderson, *J. Chem. Educ.*, **29**, 1952, 539.
43. R.T. Sanderson, "Chemical Periodicity", Reinhold Publishing Corporation, New York, 1960, p 32.
44. M. Sastry, *J. Electron Spectrosc. And Relat. Phen.*, **85**, 1997, 167.
45. V. Patil, S. Oke, M. Sastry, *J. Electron Spectrosc. And Relat. Phen.*, **85**, 1997, 249.

APPENDIX

APPENDIX

Table 1: Experimental core-ionization energies, including the date the compound was ran and the spectrometer constant.

Compound	Date	Spec. const.	Core-ionization energies (in eV)			
			C 1s	C 1s	-SF ₅ S 2p	-SO ₂ F S 2p
CF ₂ HSO ₂ F	11/20/98	0.805546	297.47			176.266
	11/23/98	0.805674	297.478			176.23
Average			297.474			176.248
Std. Dev.			0.0057			0.0255
CF ₃ SO ₂ F	2/24/97	0.807816	299.935			176.618
	2/24/97	0.807773	299.923			176.614
Average			299.929			176.616
Std. Dev.			0.0085			0.0028
(CF ₃ SO ₂) ₂ CF ₂	2/25/97	0.807454	299.218	297.037		175.049
	2/26/97	0.807595	299.282	297.102		175.194
	08/05/98	0.80553				175.305
	08/06/98	0.805576	299.391	297.113		175.294
Average			299.297	297.084		175.211
Std. Dev.			0.0875	0.0411		0.1187
CF ₃ SSCF ₃	07/09/98	0.805525	298.296		171.175	
SF ₅ CF ₃	11/2/97	0.805403	299.631		178.83	
	11/16/97	0.80544	299.674		178.877	
Average			299.653		178.854	
Std. Dev.			0.0304		0.0332	
SF ₅ SF ₅	12/17/97	0.805481			178.705	
	12/17/97	0.805507			178.72	
Average					178.713	
Std. Dev.					0.0106	
SF ₅ Br	12/17/97	0.805526	Br 3d 77.386		178.875	
	12/17/97	0.805467	77.355		178.873	
Average			77.371		178.874	
Std. Dev.			0.0219		0.0014	
SF ₅ CCH	3/11/97	0.807824	291.725		178.66	
	3/11/97	0.807724	291.703		178.579	
Average			291.714		178.62	
Std. Dev.			0.0156		0.0573	

Table 1 (cont.): Experimental core-ionization energies.

Compound	Date	Spec. const.	Core-ionization energies (in eV)			
			C 1s	C 1s	-SF ₅ S 2p	-SO ₂ F S 2p
SF ₅ CH=CH ₂	2/27/97	0.807726	291.783	289.31	NO S DATA	
	2/27/97	0.807679	291.751	289.278	NO S DATA	
	10/12/98	0.805634			178.001	
	10/17/98	0.805718			178.008	
Average			291.767	289.294	178.005	
Std. Dev.			0.0226	0.0226	0.005	
SF ₅ CH=CF ₂	12/29/97	0.805465	296.911	292.29	178.539	
	12/29/97	0.805455	296.936	292.274	178.493	
Average			296.924	292.282	178.516	
Std. Dev.			0.0177	0.0113	0.0325	
SF ₅ CF=CF ₂	10/19/97	0.80541	296.815	294.594	178.837	
	12/30/97	0.805478	296.831	294.547	178.837	
	12/30/97	0.805449	296.832	294.578	178.82	
Average			296.826	294.573	178.831	
Std. Dev.			0.0026	0.0136	0.0098	
SF ₅ CH ₂ CH ₃	12/10/98	0.805637	291.86		177.813	
	12/11/98	0.805586	291.85		177.757	
Average			291.855		177.785	
Std. Dev.			0.0071		0.0396	
SF ₅ CH ₂ CH ₂ Cl	2/27/97	0.807695	292.559	289.357	NO S DATA	
	2/27/97	0.807726	292.507	289.305	NO S DATA	
Average			292.533	289.331		
Std. Dev.			0.0368	0.0368		
SF ₅ CH ₂ CH ₂ Br	07/25/98	0.805581	292.526		177.968	
	07/28/98	0.805582	292.483		178.029	
	07/29/98	0.805579	292.429		177.999	
Average			292.479		177.999	
Std. Dev.			0.0486		0.0305	
SF ₅ CH ₂ SO ₂ F	2/18/97	0.807862	293.359		178.813	176.26
	2/19/97	0.807864	293.338		178.798	176.247
Average			293.349		178.806	176.254
Std. Dev.			0.0148		0.0106	0.0092
SF ₅ CFHSO ₂ F	2/18/97	0.807852	295.527		178.911	176.359
	2/19/97	0.807848	295.556		178.915	176.346
Average			295.542		178.913	176.353
Std. Dev.			0.0205		0.0028	0.0092

Table 1 (cont.): Experimental core-ionization energies.

Compound	Date	Spec. const.	Core-ionization energies (in eV)			
			C 1s	C 1s	-SF ₅ S 2p	-SO ₂ F S 2p
SF ₅ CF ₂ SO ₂ F	2/25/97	0.807712	297.664		178.907	176.435
	2/25/97	0.807513	297.545		178.688	176.19
	9/10/97	0.805431	297.782		178.906	176.427
	07/30/98	0.805565	297.71		178.824	176.307
	07/31/98	0.80539	297.642		178.92	176.325
Average			297.669		178.849	176.337
Std. Dev.			0.0874		0.0977	0.1004

Table 2: Experimental core-ionization energies used to determine electronegativities, their shifts relative to methane, core-ionization energies calculated using Equation 3.1, and the substituent composition of each compound. An asterisk is used to denote the central carbon where necessary. The first seven experimental ionization energies were measured in this work. The rest are from Jolly et al.²²

Compound	Ionization energy (eV) I	Shift I - I(CH ₄) (eV)	Calculated Shift (eV)	Substituents							
				F	CH ₃	CF ₃	CF ₃ SO ₂	SF ₅	FSO ₂	Cl	Br
(CF ₃ SO ₂) ₂ CF ₂	297.07	6.16	6.16	2	0	0	2	0	0	0	0
SF ₅ CF ₂ SO ₂ F	297.6	6.69	7.29	2	0	0	0	1	1	0	0
SF ₅ CHFSO ₂ F	295.54	4.63	4.64	1	0	0	0	1	1	0	0
SF ₅ CH ₂ SO ₂ F	293.34	2.43	1.99	0	0	0	0	1	1	0	0
CF ₃ SO ₂ F	299.93	9.02	9.03	3	0	0	0	0	1	0	0
SF ₅ CH ₂ CH ₃	291.9	0.99	0.82	0	1	0	0	1	0	0	0
CF ₂ HSO ₂ F	297.47	6.56	6.38	2	0	0	0	0	1	0	0
CH ₄	290.91	0	0	0	0	0	0	0	0	0	0
CH ₃ F	293.7	2.79	2.65	1	0	0	0	0	0	0	0
CH ₂ F ₂	296.44	5.53	5.31	2	0	0	0	0	0	0	0
CHF ₃	299.24	8.33	7.96	3	0	0	0	0	0	0	0
CF ₄	301.96	11.05	10.61	4	0	0	0	0	0	0	0
CH ₃ CH ₃	290.71	-0.2	-0.1	0	1	0	0	0	0	0	0
CF ₃ CH ₃	292.07	1.16	0.86	0	0	1	0	0	0	0	0
CH ₃ CF ₃	298.64	7.73	7.86	3	1	0	0	0	0	0	0
CF ₃ CF ₃	299.85	8.94	8.82	3	0	1	0	0	0	0	0
CF ₃ C*F ₂ CF ₃	297.74	6.83	7.04	2	0	2	0	0	0	0	0
CH ₃ CH ₂ F	293.39	2.48	2.56	1	1	0	0	0	0	0	0
CH ₃ CHF ₂	296.05	5.14	5.21	2	1	0	0	0	0	0	0
CClF ₃	300.31	9.4	9.35	3	0	0	0	0	0	1	0
CClH ₃	292.48	1.57	1.39	0	0	0	0	0	0	1	0
CCl ₂ F ₂	298.93	8.02	8.09	2	0	0	0	0	0	2	0
CCl ₂ H ₂	294	3.09	2.79	0	0	0	0	0	0	2	0
CCl ₃ F	297.54	6.63	6.83	1	0	0	0	0	0	3	0
CCl ₃ H	295.1	4.19	4.18	0	0	0	0	0	0	3	0
CCl ₄	296.39	5.48	5.58	0	0	0	0	0	0	4	0
CH ₃ C*H ₂ Cl	292.1	1.19	1.3	0	1	0	0	0	0	1	0
CH ₃ C*HCl ₂	293.8	2.89	2.69	0	1	0	0	0	0	2	0
CH ₃ C*Cl ₃	295	4.09	4.09	0	1	0	0	0	0	3	0
CH ₃ C*HF ₂	296.05	5.14	5.21	2	1	0	0	0	0	0	0
CF ₃ Br	299.33	8.42	8.93	3	0	0	0	0	0	0	1
CH ₃ Br	292.12	1.21	0.97	0	0	0	0	0	0	0	1
CBr ₄	294.81	3.9	3.88	0	0	0	0	0	0	0	4
CH ₃ C*H ₂ Br	291.97	1.06	0.87	0	1	0	0	0	0	0	1